crystals

MDPI

Article

Synthesis and Spectroscopic Characterization of Dapagliflozin/Zn (II), Cr (III) and Se (IV) Novel Complexes That Ameliorate Hepatic Damage, Hyperglycemia and Oxidative Injury Induced by Streptozotocin-Induced Diabetic Male Rats and Their Antibacterial Activity

Samy M. El-Megharbel [1], Eman H. Al-Thubaiti [2], Safa H. Qahl [3], Rasha A. Al-Eisa [4] and Reham Z. Hamza [4,*]

[1] Chemistry Department, College of Sciences, Taif University, P.O. Box 11099, Taif 21944, Saudi Arabia; s.megherbel@tu.edu.sa
[2] Biotechnology Department, College of Sciences, Taif University, P.O. Box 11099, Taif 21944, Saudi Arabia; i.althubaiti@tu.edu.sa
[3] Biology Department, College of Sciences, Jeddah University, Jeddah 21959, Saudi Arabia; shqahal@uj.edu.sa
[4] Biology Department, College of Sciences, Taif University, P.O. Box 11099, Taif 21944, Saudi Arabia; r.hasan@tu.edu.sa
* Correspondence: reham.z@tu.edu.sa

check for updates

Citation: El-Megharbel, S.M.; Al-Thubaiti, E.H.; Qahl, S.H.; Al-Eisa, R.A.; Hamza, R.Z. Synthesis and Spectroscopic Characterization of Dapagliflozin/Zn (II), Cr (III) and Se (IV) Novel Complexes That Ameliorate Hepatic Damage, Hyperglycemia and Oxidative Injury Induced by Streptozotocin-Induced Diabetic Male Rats and Their Antibacterial Activity. *Crystals* **2022**, *12*, 304. https://doi.org/10.3390/cryst12030304

Academic Editors: Assem Barakat, Alexander S. Novikov and Venu Vangala

Received: 17 January 2022
Accepted: 12 February 2022
Published: 22 February 2022

Publisher's Note: MDPI stays neutral with regard to jurisdictional claims in published maps and institutional affiliations.

Abstract: Diabetes mellitus (DM) causes an imbalance in the oxidative status of the human body. Three novel Dapagliflozin (Dapg) Zn (II), Cr (III) and Se (IV) complexes were prepared and characterized by elemental analysis, IR, electronic spectra, magnetic susceptibility, scanning electron microscopy (SEM) and X-ray diffraction. The molar conductance values confirmed the non-electrolytic nature of the Dapg complexes. According to spectral data, Dapg acts as a bidentate ligand. The thermal analyses of the complexes were studied using the DSC technique. The surface morphology and particle sizes of the Dapg complexes were investigated using SEM and XRD. XRD confirmed the crystalline structure for the complexity. This study investigated the effect of novel metal complexes of Dapg with the metals Zn (II), Cr (III) and Se (IV) on oxidative injury and tissue damage in the hepatic tissue of streptozotocin (STZ)-induced diabetic male rats. DM was experimentally induced in male rats. The diabetic rats received Dapg, Dapg/Zn, Dapg/Cr and Dapg/Se orally for 30 successive days. Male rats exposed to STZ showed multi-histopathological alterations in their hepatic tissue, including inflammatory and structural changes. STZ elevated oxidative stress markers in the hepatic tissue and lowered the antioxidant defense enzymes. Supplementation of Dapg with Zn, Cr or Se novel complexes significantly prevented hepatic injury and suppressed the generation of reactive oxygen species. The Dapg/Zn complex was highly effective against *Bacillus subtilis* and *Streptococcus penumonia*, while Dapg/Cr was highly effective against *Escherichia coli* and *Pseudomonas aeruginosa*, and Dapg/Se was highly effective against *Staphylococcus aureas*. In conclusion, Dapg novel metal complexes with Zn, Cr or Se protect against oxidative injury and the pathophysiological and bacterial complications of DM and hepatic tissue injury. The Dapg novel metal complexes improved hepatic functions, reduced blood glucose levels and enhanced the levels of antioxidant defense enzymes in diabetic male rats.

Keywords: drug metal complexes; dapagliflozin; chromium; oxidative stress; hepatic tissues

1. Introduction

Diabetes mellitus (DM) increases the rate of mortality and poses a huge burden on the economy. Globally, it is reported that approximately 4–4.6 million patients with diabetes die annually. At present, diabetes is a high-incidence chronic disease worldwide [1].

Diabetes is a disease that impairs the body's ability to control blood glucose levels. Diabetes can lead to an excessive level of sugar in the blood, which culminates in adverse

pathophysiological complications, including hepatic toxicity, heart failure and kidney failure [2].

Patients with DM often have other complications, such as gastric dysfunction, insomnia and even dyslipidemia [1].

SGLT2 inhibitors are listed as a new class of oral anti-hyperglycemic medications for the pharmacological management of DM [3]. Sodium-glucose co-transporter 2 (SGLT2) inhibitors cause the kidney tissues to increase urinary glucose excretion and inhibit the hyperglycemic state, thus improving glycemic control [4]. In addition, SCLT2 targets the improved function of β-cells and increases insulin sensitivity [5].

Several categories of antidiabetic drugs are used for the treatment of diabetic patients for lowering blood glucose. Dapagliflozin (Dapg) is a member of the SGLT2 drug category. The chemical structures of Dapg are shown in Figure 1. Dapg is a glucose-lowering agent used in the treatment of diabetics. It is a known inhibitor of SGLT2. By inhibiting the receptor of transporter protein known as SGLT2 in the kidney, it causes a decline in glucose reabsorption in the renal tissue, which leads to excessive urinary excretion and a decline in blood glucose levels [1].

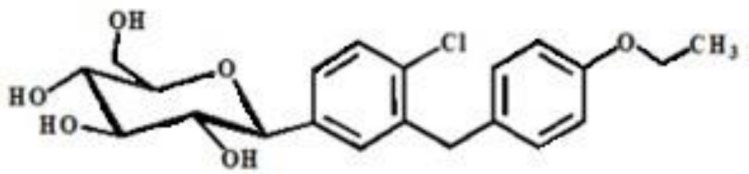

Figure 1. Chemical structure of Dapagliflozin (Dapg).

Dapg, which is the third member of the gliflozin family, has pronounced cardioprotective and neuroprotective effects in the development of insulin resistance in animals. Dapg has been shown to restore the declined mitochondrial membrane potential responsible for mitochondrial dynamics, as well as providing a marked increment in Ca^{2+} homeostasis in tested cardiomyocytes in diabetic rats [6]. Dos Santos and Filho [7] treated patients with nonalcoholic fatty liver disease with a fixed dose of 10 mg of Dapg for an average of 75 days. Liver enzymes ALT and AST, insulin hormone, insulin resistance level "HOMA-IR" and weight levels were significantly reduced after treatment, with no reports of its effect on the hepatic ecostructure.

Chromium (Cr III) is required in a small amount to maintain the vitality of the human body [1]. Cr is among the most important trace elements that the body can absorb. It is reported that Cr is the most essential stable form that can be accumulated in soft tissues, such as the liver and bone. It plays a vital role in the metabolism of both lipids and carbohydrates. It may elevate insulin sensitivity in the human body and can also inhibit cholesterol synthesis in hepatic tissues. Cr deficiency is reported to cause hypercholesterolemia and DM complications [8].

Zinc (Zn) is an essential trace element that plays a vital role in cellular metabolism. Zn is essential for enzymatic processes. Its deficiency may result in a wide spectrum of declining drug elimination, clinical manifestations and immune dysfunction [9]. The liver tissue is the main target organ that is responsible for zinc metabolism and it can be affected by hepatic diseases. Moreover, Zn deficiency may change the functions of hepatocytes and can result in several liver diseases and bacterial infections [10].

Selenium (Se) is shown to be reduced in patients with chronic liver diseases [11]. Se is an essential trace element for humans [12]; it is essential for the antioxidant defense system [13]. It was previously reported that the biosynthesis of selenoproteins is greatly affected in hepatic encephalopathy [14].

Currently, SGLT2 inhibitors are approved as good treatments for type II DM and Dapg is one of these categories of drugs and also has a good impact on hepatic enzyme levels. Without studying histological alterations in the hepatic tissues, Hazem et al. [15]

reported that Dapg treatment protected the liver tissues against steatohepatitis in diabetes via inhibiting oxidative stress, inflammation and fibrosis progression. Meanwhile, the effects of Dapg with novel metal complexes on hepatic injury and metabolism and liver histological structure have not been illustrated before.

Liuran et al. [16] demonstrated that Dapg ameliorates hepatic steatosis by reducing lipogenic enzymes while inducing autophagy via the AMPK-mTOR pathway and thus improves hepatic functions and reduces hepatic lipid accumulation.

Therefore, this study aimed to investigate whether Dapg alone or its novel metal complexes (Zn, Cr and Se) could improve hepatic function parameters and insulin resistance in STZ-induced diabetic male rats and to assess the ameliorative role of complexes of metal ions Cr, Zn and Se with Dapg to enhance the hepatic functions.

2. Materials and Methods

2.1. Chemicals

Analytical-grade chemicals, solvents, zinc (II) chloride, chromium (III) chloride, selenium (IV) chloride and Dapagliflozin drug (purity 99%) were purchased from commercial suppliers (Sigma-Aldrich, St. Louis, MO, USA) and used for all experimental purposes without further purification.

2.2. Synthesis of Zinc (II), Chromium (III) and Selenium (IV) Complexes with Antidiabetic Drug (Dapaglifozin)

The zinc (II)–, Cr (III)– and selenium (IV)–Dapagliflozin complexes were synthesized by dissolving Dapagliflozin (1 mmol, 0.41 g) in 20 mL of methanol and then mixing with 1 mmol $ZnCl_2$, $CrCl_3 \cdot 6H_2O$ and $SeCl_4$ in 20 mL CH_3OH solution. The mixtures were heated at 80 °C with continuous stirring for 4 h. The mixtures were left to precipitate for 12 h, as with our previous experimental work preparation [12].

2.3. Characterization of Synthesized Zinc, Chromium and Selenium Dapagliflozin Complexes

2.3.1. Differential Scanning Calorimetry (DSC)

The change in properties for zinc (II), Cr (III) and selenium (IV) complexes were investigated using differential scanning calorimetry (DSC) (DSC60, Shimadzu, Japan). The temperature ranged up to 350 °C and the rate of temperature was 10 °C/min at a flow rate of 20 mL/min under a N_2 gas atmosphere.

2.3.2. Infrared Spectrophotometry (FTIR)

The FTIR analyses for zinc (II), chromium (III) and selenium (IV) complexes were carried out using an infrared Bruker spectrophotometer in the range of 400–4000 cm^{-1}.

2.3.3. Conductance Measurements

The conductance measurements with a concentration of 10^{-3} mmol/L for the synthesized zinc (II), chromium (III) and selenium (IV) complexes in DMSO solvent were performed using the HACH conductivity meter model.

2.3.4. Electronic Absorption Spectra

UV for zinc (II), chromium (III) and selenium (IV) complexes was recorded in DMSO solvent within the range of 800–200 nm using a UV2 Unicam UV/Vis Spectrophotometer fitted with a quartz cell of 1.0 cm path length.

2.3.5. X-ray Diffraction

The X-ray diffraction patterns for zinc (II), chromium (III) and selenium (IV) were recorded on X 'Pert PRO PANanalytical X-ray powder diffraction equipment, targeting copper with secondary monochromate.

2.3.6. Scanning Electron Microscopy

The surface morphologies for particles of zinc (II), chromium (III) and selenium (IV) complexes were carried out using a Quanta FEG 250 scanning microscope (SEM).

2.4. Experimental Animals

Sixty mature male rats (two months age), weighing 160–170 g, were kept in sensitized metal cages with free access to food ad libitum and water at a room temperature of 25 ± 2 °C within a 12 h light/dark cycle. Rats were left to acclimatize for 2 weeks before the experiment. The experimental protocol was approved by the Deanship of Scientific Research at Taif University Ethical Committee, with approval number 42-0074. Rats were sacrificed under light ketamine/xylazine anesthesia, and every effort was made to reduce stress and pain. Animals involved in the experiment were fed high-fat diets for around 4 weeks before the start of the experiment to mimic type II diabetes, based on study [17]; then, experimental diabetes mellitus was induced by a single injection of STZ, as explained in detail in the next section.

Male rats were divided into 6 groups. Group I, the control group, was administered gum acacia as a vehicle. Group II, the STZ group, was given a single dose of STZ (50 mg/kg) by (I.P) injection [17]. Group III was a diabetic group given STZ and orally administrated 3 mg/kg of Dapg drug [15]. Groups IV, V and VI were the diabetic groups treated with STZ followed by oral administration of the same doses, 3 mg/kg, of Dapg/Cr, Zn and Se complexes, respectively, as shown in the experimental protocol (Figure 2).

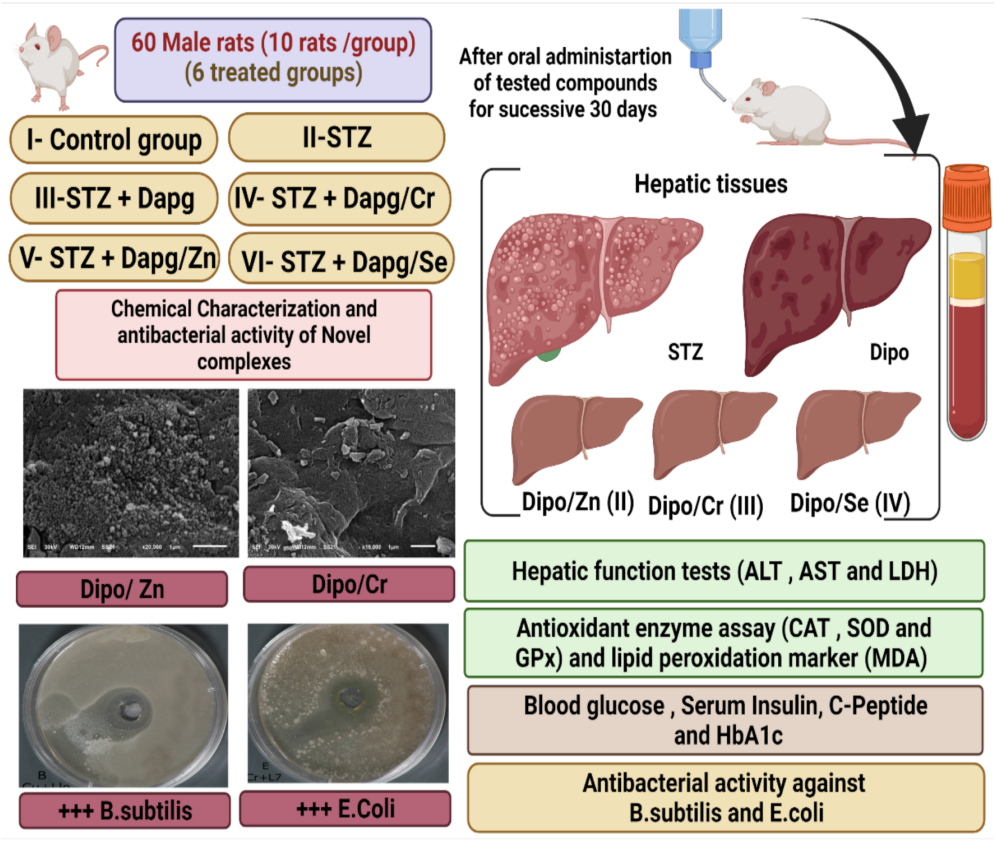

Figure 2. The experimental design and processes of the experiment.

2.5. Experimental Induction of DM

Freshly prepared STZ dissolved in phosphate-buffered saline (pH = 4.5) was used to induce diabetes in male rats. STZ (50 mg/kg) (I.P), which was freshly prepared in the early morning, was administered by intraperitoneal injection to male rats that had fasted for 6 h [17] following the administration of high-fat feed (composed of 66.5% commercial feed, 13.5% artificial butter and 20% sugar) for three weeks prior to the experimental induction of DM by a single injection of STZ [18]. Seventy-two hours after STZ injection, blood glucose levels were measured to evaluate the diabetic status of the animals. Subjects with blood glucose levels higher than 280 mg/dL were considered diabetic, as shown in the experimental protocol (Figure 2).

2.6. Blood Collection

Using capillary tubes, blood samples were collected from the eye plexus with light anesthesia for biochemical and physiological analyses. The rats were ethically decapitated. Hepatic tissue samples were kept at −25 °C.

2.7. Determination of the Fasting Blood Glucose Level

Fasting blood glucose levels were evaluated using commercial kits (Bio-Diagnostic Co.).

2.8. Measurements of Serum Insulin, C-Peptide and HbA1c

Serum insulin was evaluated using a rat ELISA kit (ALPCO Diagnostics). We used the C-peptide enzyme commercial immune assay (Sigma-Aldrich) and HbA1c kits according to the manufacturers' protocols.

2.9. Hepatic Function Activities and Biomarkers

ALT, AST and ALP levels were assessed by using (SENTINEL CH) kits. LDH levels were measured in accordance with the manufacturer's instructions.

2.10. Preparation of Hepatic Tissue Homogenates for the Determination of the Redox State

Small liver portions from hepatic tissues were used to determine oxidative injury. The tissues were immersed in 50 mmol phosphate buffer (pH 7.4); then, a protease inhibitor was added for the protection of enzymes from oxidation, and samples were centrifuged to obtain the supernatant of tissue homogenates.

2.11. Determination of Oxidative Stress Biomarker Activities in Hepatic Tissues

The MDA level was determined following the method of Ohkawa et al. (1979) [19]. SOD activity was determined using the technique of Marklund and Marklund (1974) [20]. CAT activity was estimated by applying the method of Aebi (1984) [21]. GRx was determined following Couri and Abdel-Rahman (1980) [22]. Glutathione peroxidase (GPx) was assayed using the technique of Hafeman et al. (1974) [23].

2.12. Histological Changes

Small hepatic tissue samples were fixed in 10% buffered formalin for further histological examination [24].

2.13. Antibacterial Activities of Dapg and Its Metal Complexes

The antimicrobial activity of the tested samples was determined by a modification of the Kirby–Bauer disc diffusion method [25]. Antibacterial activity was tested in triplicate and then the mean was calculated. In brief, 100 µL of the best bacteria was grown in 10 mL of fresh media until they reached a count of approximately 108 cells/mL [26]. Then, 100 µL of the microbial suspension was spread onto agar plates corresponding to the broth in which they were maintained. Isolated colonies of each organism that may play a pathogenic role were selected from the primary agar plates and tested for susceptibility by the disc diffusion method [27].

Plates were inoculated at 25 °C for 48 h. The Gram (+) bacterium *Bacillus subtilis* and the Gram (−) bacterium *Escherichia coli* were incubated at 35–37 °C for 24–48 h. Afterwards, the diameters of the inhabitation zones were measured in millimeters [28]. Standard discs of tetracycline (antibacterial agent) served as positive controls for the antimicrobial activity, and a filter disc impregnated with 10 µL solvent (dist. H_2O, chloroform, DMSO) was used as a negative control.

The agar used was the Mueller–Hinton agar, which was tested continuously in terms of its pH. Further, the depth of the agar in the plate was a factor considered in the disc diffusion method. If an organism is placed on the agar, it will not grow in the area around the disc if it is susceptible to the chemical. The area of no growth around the disc is called the 'zone of inhibition' or 'clear zone'. For the disc diffusion, the zone diameters were measured with slipping calipers from the National Committee for Clinical Laboratory Standards [29]. Agar-based methods, such as the Etest disc diffusion, can be good alternatives because they are simpler and faster to perform than the broth methods [30].

2.14. Statistical Analysis

Data were expressed as mean ± standard error of the mean and analyzed by one-way analysis of variance using the SPSS v.22 program (SPSS Inc., Chicago, IL, USA). The significance of the mean differences was examined using the Duncan post hoc test [31].

3. Results

3.1. Molar Conductance Data

Dapg complexes have high stability at room temperature and high solubility in DMSO with slight warming. The molar conductance data for Zn (II), Cr (III) and Se (IV) Dapg complexes are 34, 68 and 79 µs/cm, respectively. According to the conductance values of Cr (III) and Se (IV) complexes, there are one or two Cl^- anions outside the chelation sphere [32]. According to the conductance values, the chromium (III) complex has 68 µs/cm, and the selenium (IV) complex has conductance equal to 79 µs/cm. This may be attributed to the presence of one Cl^- anion outside the chelation sphere for the Cr (III) complex, Meanwhile, there are two ions, with one ion representing the chelation sphere. Meanwhile, for the Se (IV) complex, there are two Cl^- anions outside the chelation sphere and thus the total number of ions is three, and the conductance value increases upon increasing the total number of ions [32]. By adding silver nitrate, a white precipitate is formed, which confirms the presence of chloride ions. The molar conductance for the Zn (II)–Dapg complex at 34 µs/cm and 25 °C showed that Zn (II) is non-electrolytic.

3.2. Thermal Analysis

The changes in phase for Dapg and its Zn, Cr and Se complexes were investigated by differential scanning calorimetry. Dapg showed an endothermal peak at 77.98 °C, while Zn (II)–, Cr (III)– and Se (IV)–Dapg complexes showed different peaks at 110 °C, 108.79 °C and 115.58 °C, respectively, thereby confirming the formation of new complexes.

3.3. Infrared

Fourier-transform infrared spectroscopy was used to characterize the stretching and molecular vibration of Dapg, which helped in the identification of the main functional groups of Dapg. By comparison with Zn (II), Cr (III) and Se (IV) Dapg complexes, the main sites of Dapg electron donation were confirmed. If the pure Dapg drug and its complex produced the same infrared spectroscopy (IR), it could be concluded that no new compounds were formed, whereas any disappearance or peak shifts confirm the formation of a new Dapg complex. The IR of pure Dapg and its Zn, Cr and Se complexes are shown in (Figure 3).

For IR of the free Dapagliflozin ligand, the assignments for stretching vibrational bands have been explained [33] as follows: the band appearing at 2940 cm^{-1} is due to the vibrational stretching motion of aliphatic (C–H). The vibration bands appearing

at 1100–11,050 cm^{-1} are assigned to ν (C–O). The stretching vibration bands present at 1550–1450 cm^{-1} are assigned to ν (C=C) aromatic rings. The bands appearing at 1300–1200 cm^{-1} are assigned to (δ (C–O–H)); moreover, for the Dapagliflozin ligand, the characteristic stretching vibration for OH is observed at 3282 cm^{-1} [34], while this peak is shifted to 3294, 3295 and 3292 cm^{-1} for the Zn, Cr and Se Dapagliflozin complexes, respectively. For the zinc, chromium and selenium Dapagliflozin complexes, new bands appeared at 419, 523 and 518 cm^{-1}, characteristic of ν (M-O) [35,36]. These changes in the IR absorption spectra confirm the chelation between the Dapagliflozin drug and metal ions.

For the IR of free Dapg, the characteristic stretching vibration for OH is observed at 3282 cm^{-1} [33], whereas this peak is shifted to 3294, 3295 and 3292 cm^{-1} for the Zn, Cr and Se Dapg complexes, respectively. The Zn, Cr and Se Dapg complexes showed new bands at 419, 523 and 518 cm^{-1}, which corresponded to the M-O vibration mode [34,35]. These changes in the IR confirm the chelation between Dapg and the metal ions.

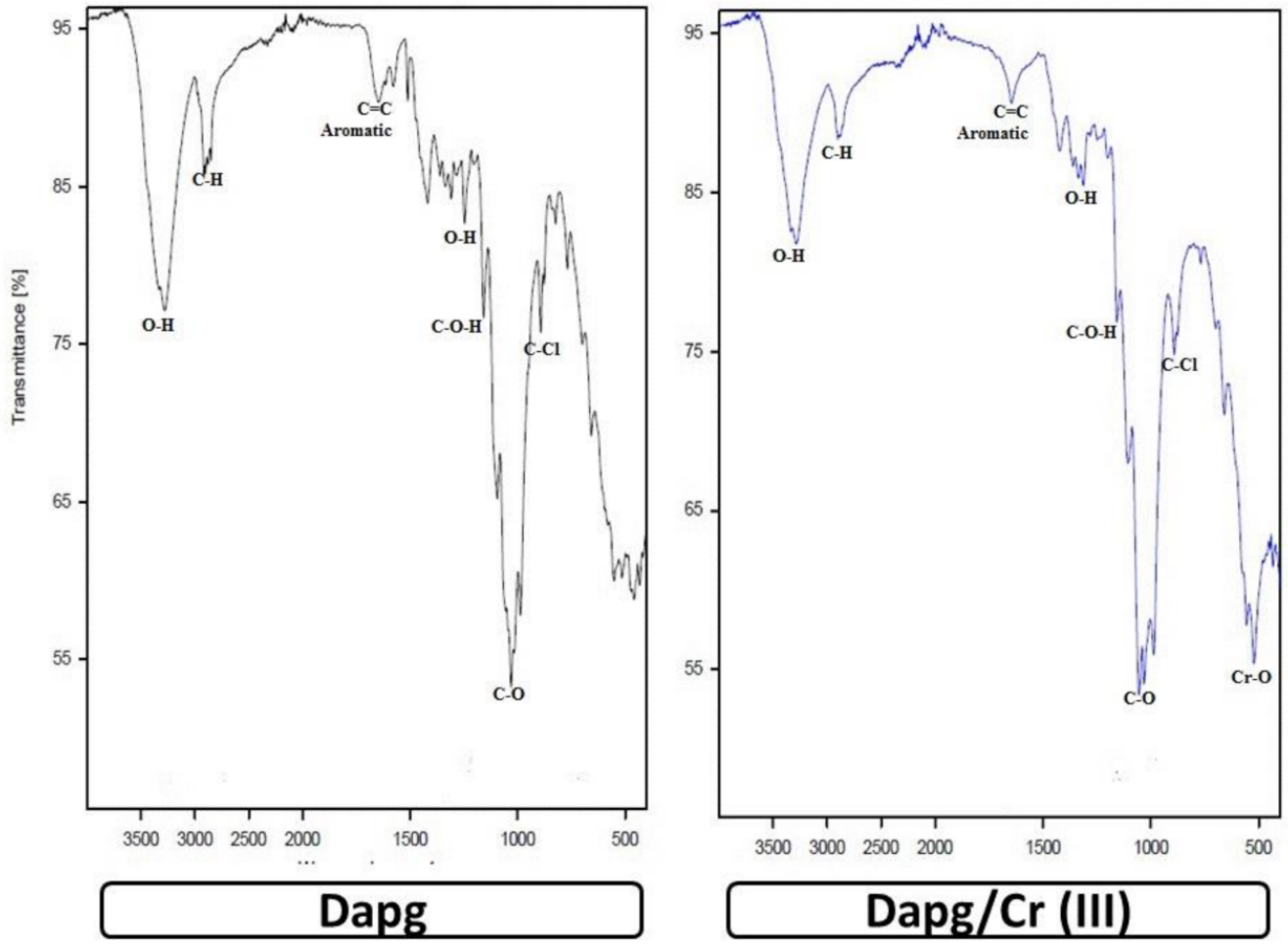

Figure 3. *Cont.*

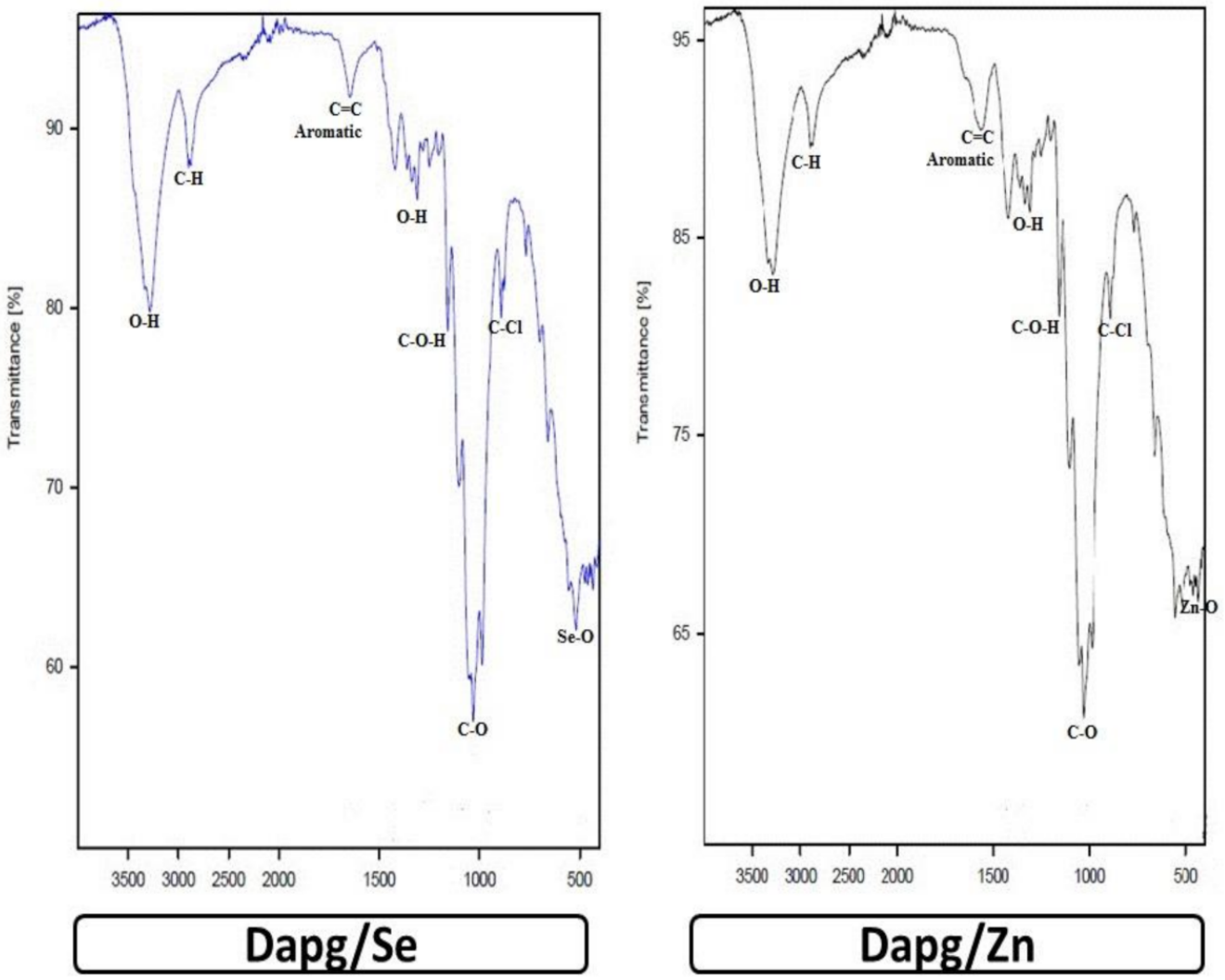

Figure 3. FT-IR of Dapg, Cr–Dapg, Zn–Dapg and Se–Dapg.

3.4. Electronic Spectra and Magnetic Measurements

For Dapg, two essential UV bands appeared at 230 and 275 nm (Figure 4), which refer to $\pi \rightarrow \pi^*$, for the aromatic ring and the OH and CH_3 groups [36] (Figure 4). For Zn (II) and Se (IV), they appeared at 275 and 335 nm, while for Cr (III), they appeared at 275 and 395 nm, which confirms the chelation of metal ions with Dapg (Figure 4). For the Cr (III) complex, the peaks appeared at 510, 670 and 795 nm, which refer to the metal–ligand charge transfer complex. The value of the magnetic moment for the Cr (III)–Dapg complex lies at 3.79 BM, which corresponds to an octahedral field [37].

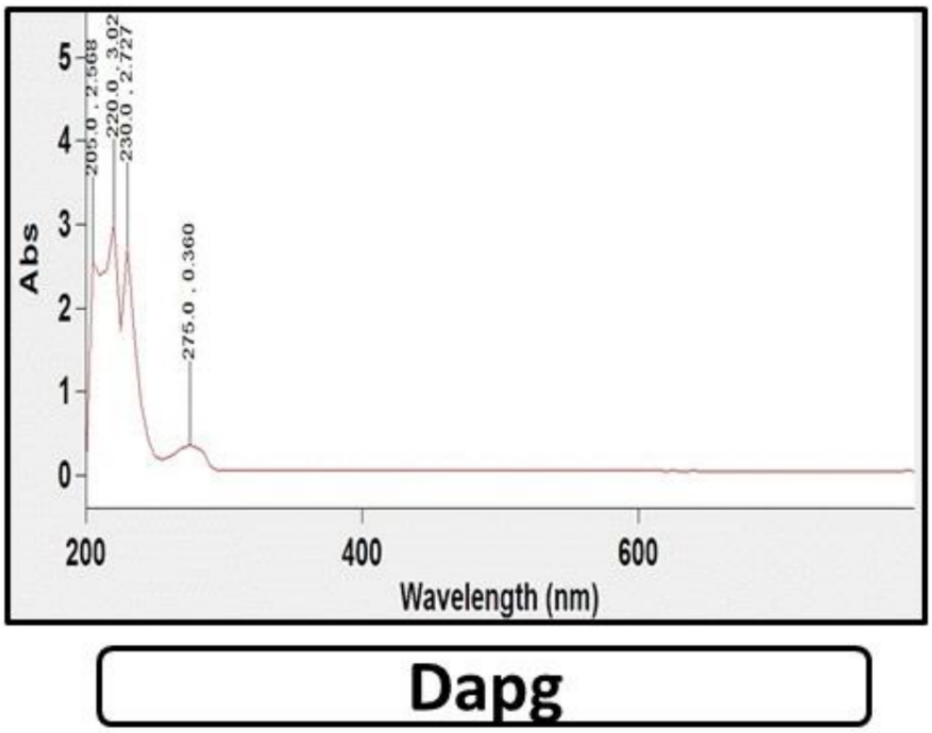

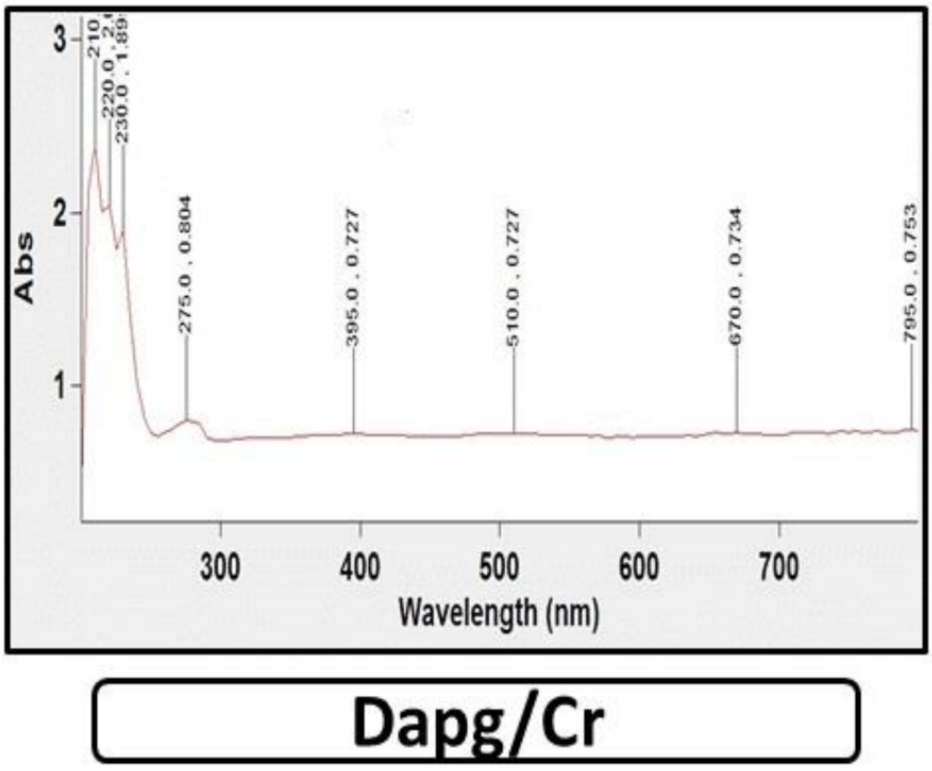

Figure 4. *Cont*.

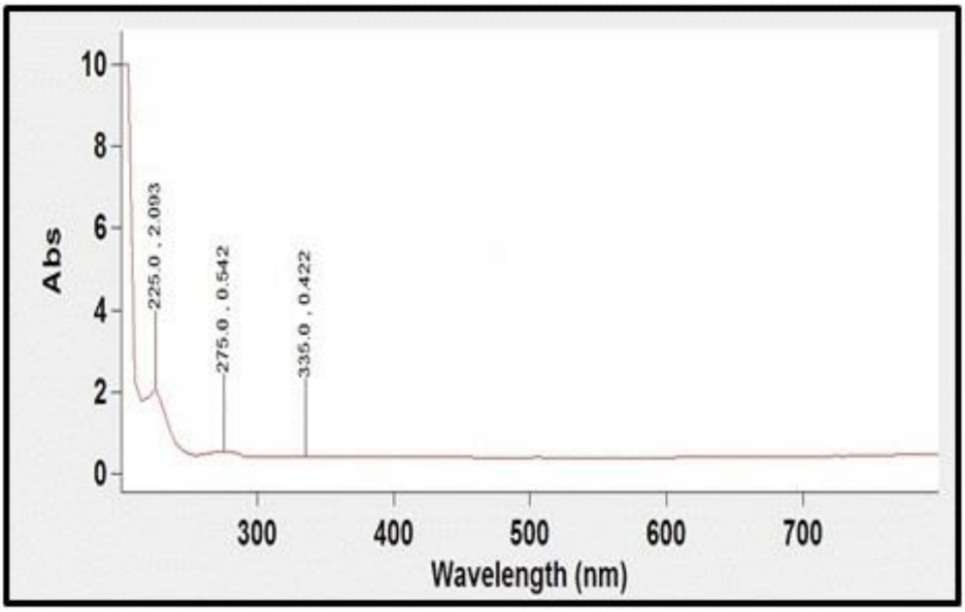

Dapg/Se

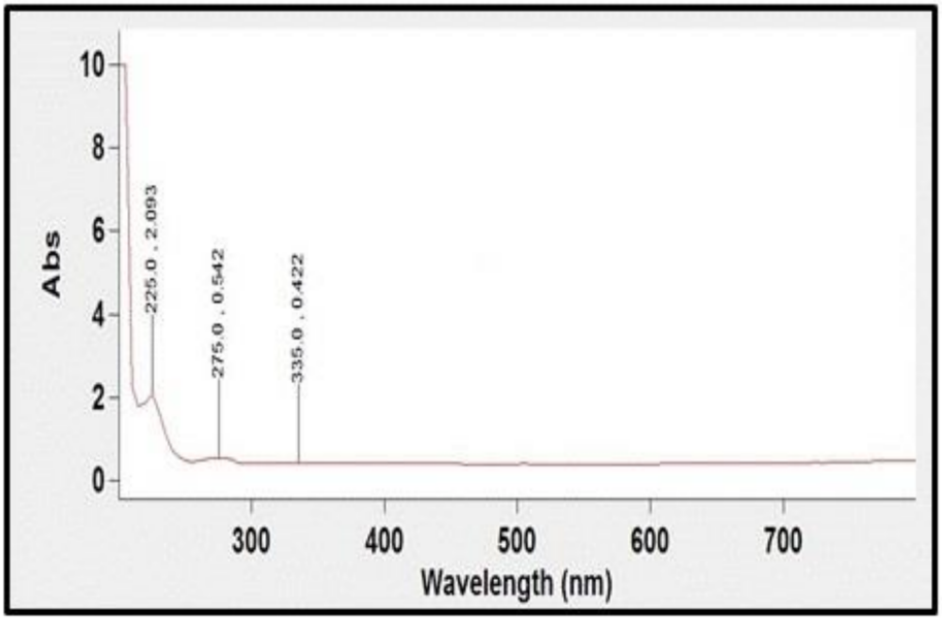

Dapg/Zn

Figure 4. UV of Dapg, Cr–Dapg, Zn–Dapg and Se–Dapg.

3.5. X-ray Diffraction (XRD)

XRD analysis was used to investigate the crystalline structure of Dapg and its metal complexes at room temperature using Cu Kα radiation. For the synthesized Dapg metal complexes, the XRD patterns show that they are crystalline in nature [38]. The diffractograms of Zn (II), Cr (III) and Se (IV) give a sharp and strong Braggs diffraction line. The Zn (II)–, Cr (III)– and Se (IV)–Dapg complexes showed two sharp lines at 2θ of (28, 31), (26, 28) and (27, 31), respectively. For the synthesized complexes, the crystalline size was calculated using the Scherrer formula [39,40] $D = k\lambda/\beta Cos\theta$, where k is a constant (0.94), λ is the wavelength of the X-ray used (0.154 nm), and β is the full width at half maxima peak of the XRD pattern. The crystalline size for Zn, Cr and Se complexes was found to be 65, 78 and 72 nm, respectively.

3.6. Scanning Electron Microscopy (SEM)

The images of SEM for the Dapg complexes are shown in Figure 5. The surface morphology changed according to the metal ions; some images contained a large number of irregular shapes, and some images contained regular grains. It is quite clear from the results that the average grain size estimated by SEM was significantly larger than the average grain size measured by XRD.

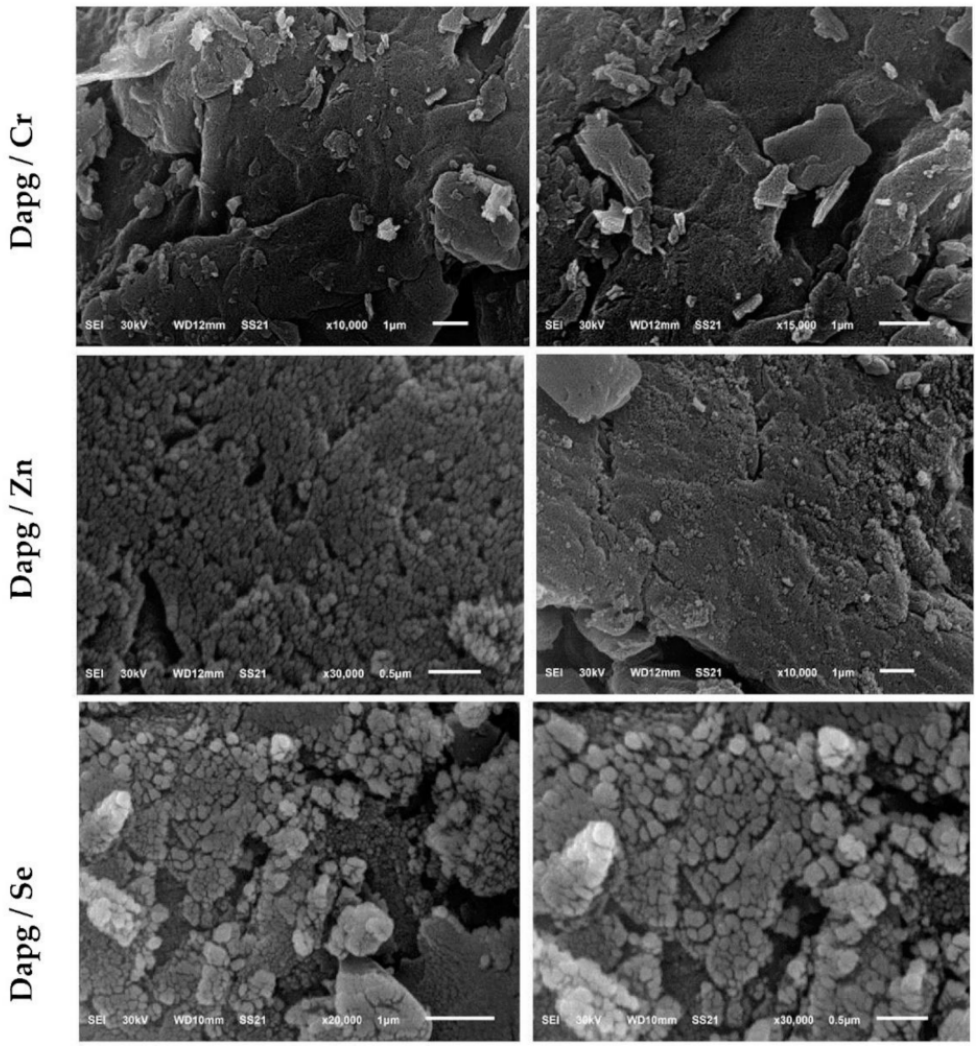

Figure 5. SEM image of Dapg complexes (Cr–Dapg, Zn–Dapg and Se–Dapg).

3.7. Antibacterial Activity Evaluation

Biological evaluations were performed in terms of the antimicrobial activities of the target compounds against Gram-positive (*Bacillus subtilis*, *Streptococcus pneumonia* and *Staphylococcus aureus*) and Gram-negative (*Escherichia coli* and *Pseudomonas aeruginosa*) bacteria. Results from the agar disc diffusion tests for the antimicrobial activities of the target compounds are presented in Table 1 and illustrated in Figure 6. The diameters of the zone of inhibition (in mm) of the standard drug tetracycline against Gram-positive bacteria *B. subtilis* and *S. aureus* and Gram-negative bacteria *E. coli* and *P. aeruginosa* were found to be 36, 30, 31 and 35 mm, respectively. Under identical conditions, Table 1 and Figure 6 show that all complexes were found to be efficient, with high antimicrobial activity.

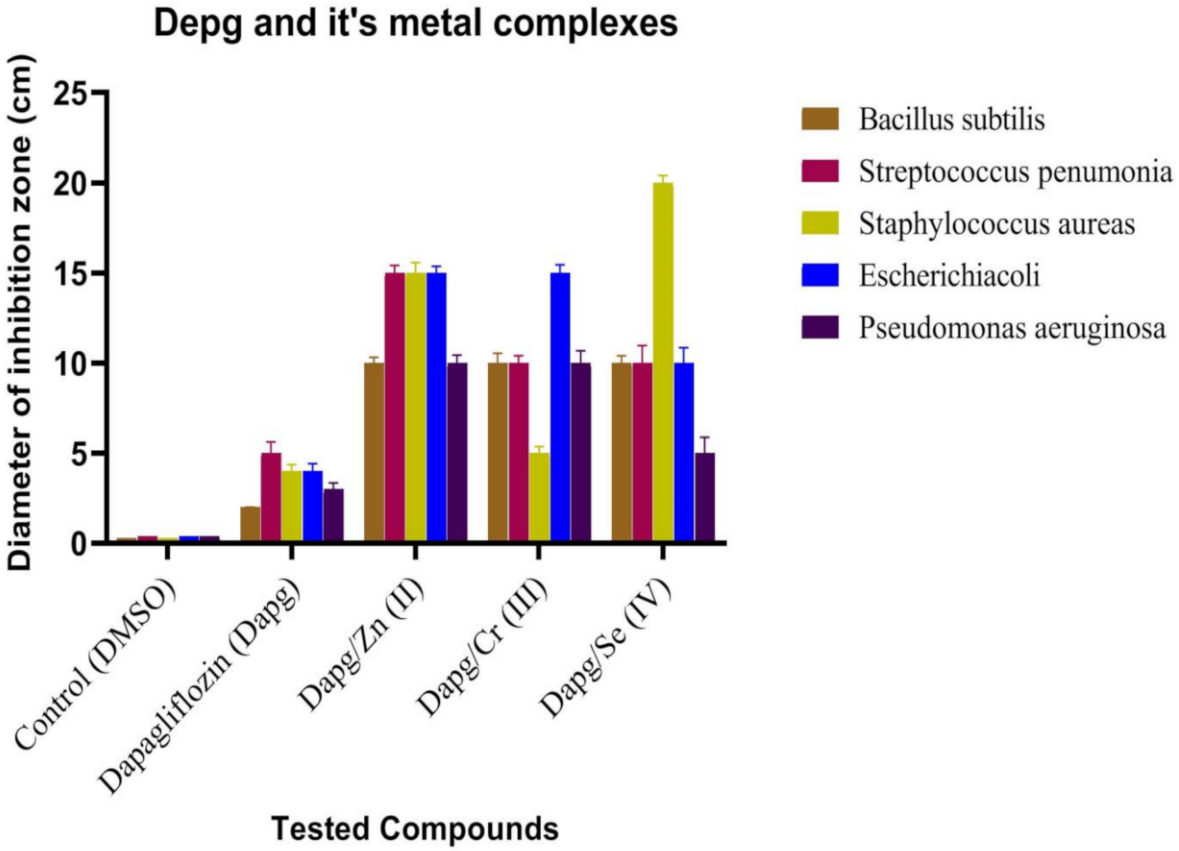

Figure 6. Antibacterial activity of Dapg and Zn (II)–, Cr (III)– and Se (IV)–Dapg metal complexes.

Table 1. Inhibition zone diameter (mm/mg sample) of Dipogliflazone and the complexes.

Sample	Inhibition Zone Diameter (mm/mg Sample)				
	Bacillus subtilis **(G^+)**	***Streptococcus penumonia*** **(G^+)**	***Staphylococcus aureas*** **(G^+)**	***Escherichia coli*** **(G^-)**	***Pseudomonas aeruginosa*** **(G^-)**
Control (DMSO)	0.0 ± 0.0^{c}	0.0 ± 0.0^{d}	0.0 ± 0.0^{e}	0.0 ± 0.0^{d}	0.0 ± 0.0^{d}
Dipogliflazone (Depg)	2 ± 0.01^{b}	5 ± 0.63^{c}	4 ± 0.36^{d}	4 ± 0.41^{c}	3 ± 0.35^{c}
Zn (II)–Dapg	10 ± 0.32^{a}	15 ± 0.41^{a}	15 ± 0.58^{b}	15 ± 0.36^{a}	10 ± 0.45^{a}
Cr (III)–Dapg	10 ± 0.54^{a}	10 ± 0.41^{b}	5 ± 0.36^{c}	15 ± 0.45^{a}	10 ± 0.69^{a}
Se (VI)–Dapg	10 ± 0.41^{a}	10 ± 0.98^{b}	20 ± 0.41^{a}	10 ± 0.85^{b}	5 ± 0.88^{b}

Means within the same column (mean ± SE) carrying different letters are significant at $p \leq 0.05$ using Duncan's multiple range test, where the highest mean value has symbol (^{a}) and those decreasing in value are assigned alphabetically.

3.8. Blood Glucose, Insulin and Fasting C-Peptide Levels

STZ elevated the fasting blood glucose levels, which was accompanied by a marked decline in insulin levels and serum fasting C-peptides in the STZ group as compared to the control group. As shown in Table 2, the group treated with STZ and Dapg displayed a non-marked elevation in blood glucose levels. They also demonstrated a significant decline in blood glucose levels, which was accompanied by the elevation of insulin and serum fasting C-peptide levels, as compared with the diabetic untreated group.

Table 2. Fasting blood glucose level, insulin hormone, HBA1C and fasting serum C-peptide results.

Groups	Fasting Blood Glucose (mg/dL)	Insulin Hormone (uIU/mL)	HbA1C (mmol/mol)	Fasting Serum C-Peptide (ng/mL)
Control group	80.81 ± 1.25^{e}	$25.86 \pm 2.15^{a,b}$	3.12 ± 0.75^{d}	3.88 ± 0.19^{a}
STZ group	351.29 ± 8.02^{a}	4.70 ± 0.84^{d}	$10.41 \pm 1.26^{a,b}$	0.22 ± 0.05^{d}
STZ plus Dapg group	120.96 ± 6.03^{b}	19.36 ± 2.85^{c}	5.02 ± 1.82^{b}	2.99 ± 0.87^{c}
STZ plus Cr–Dapg group	109.16 ± 4.75^{c}	23.03 ± 2.11^{c}	$7.01 \pm 0.87^{c,d}$	3.76 ± 0.27^{b}
STZ plus Zn–Dapg group	102.26 ± 3.75^{c}	21.03 ± 2.91^{c}	$5.01 \pm 0.77^{c,d}$	3.71 ± 0.77^{b}
STZ plus Se–Dapg group	$92.27 \pm 4.26^{d,e}$	21.75 ± 1.02^{b}	5.54 ± 0.66^{d}	4.10 ± 0.76^{a}

Means within the same column (mean ± SE) carrying different letters are significant at $p \leq 0.05$ using Duncan's multiple range test, where the highest mean value has symbol ([a]) and those decreasing in value are assigned alphabetically.

3.9. Oxidative Stress Biomarkers

Table 3 shows that experimental DM induced by STZ afforded a significant decline in catalase (CAT), superoxide dismutase (SOD) and glutathione peroxidase (GPx) antioxidant enzymes, while affording a highly significant elevation of the malondialdehyde (MDA) level. Diabetic groups treated with novel complexes of Cr–Dapg, Zn–Dapg and Se–Dapg showed a marked elevation of CAT, SOD and GPx levels and a significant decline in MDA levels. The group treated with Dapg in conjunction with Cr presented the best results.

Table 3. Oxidative/antioxidant parameters of antioxidant enzymes in hepatic tissue of male rats.

Groups	Hepatic CAT (U/g)	Hepatic SOD (U/g)	Hepatic MDA (U/g)	Hepatic GPx (U/g)
Control group	1.88 ± 0.21^{a}	$22.05 \pm 1.15^{a,b}$	3.05 ± 0.48^{e}	34.05 ± 1.85^{a}
STZ group	0.26 ± 0.10^{d}	5.22 ± 1.35^{d}	81.15 ± 0.96^{a}	7.56 ± 1.18^{e}
STZ plus Dapg group	1.42 ± 0.36^{c}	19.91 ± 1.58^{c}	20.42 ± 1.02^{b}	23.15 ± 1.15^{d}
STZ plus Cr–Dapg group	1.63 ± 0.48^{b}	20.52 ± 2.16^{b}	12.26 ± 1.45^{c}	26.41 ± 1.28^{c}
STZ plus Zn–Dapg group	1.74 ± 0.22^{a}	21.19 ± 2.25^{b}	8.78 ± 1.25^{d}	$31.58 \pm 1.58^{b,c}$
STZ plus Se–Dapg group	1.88 ± 0.21^{a}	$22.05 \pm 1.15^{a,b}$	3.05 ± 0.48^{e}	34.05 ± 1.85^{a}

Means within the same column (mean ± SE) carrying different letters are significant at $p \leq 0.05$ using Duncan's multiple range test, where the highest mean value has symbol ([a]) and those decreasing in value are assigned alphabetically.

3.10. Histological Examination

Results showed that STZ caused significant degeneration in the hepatic structure, as well as increased eosinophilia, granular cytoplasm with hemorrhage and necrotic nuclei. Meanwhile, treatment of different groups with the novel metal complexes of Dapg led to the significant amelioration of hepatic tissue with mild toxicity, including some ballooning of hepatocytes and necrotic nuclei as shown in Figure 7.

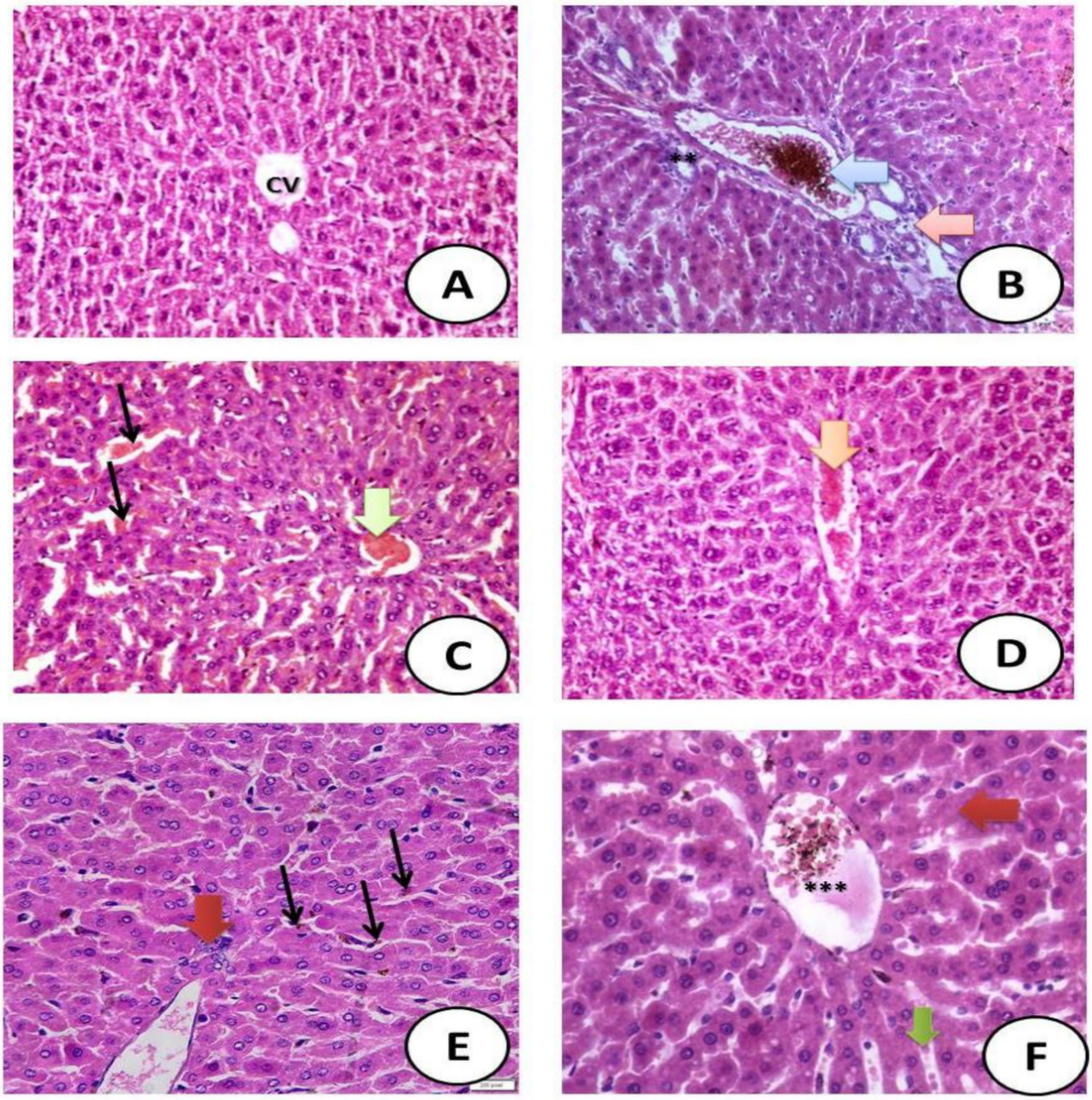

Figure 7. Histological sections. (**A**) Control group showing normal hepatic structure with normal-sized central vein (CV) (H&EX400). (**B**) STZ-treated group showing severe hepatic toxicity in the form of hypertrophy of hepatocytes with appearance of binucleated hepatocytes and increased eosinophilia, granular cytoplasm (Blue arrow) and vesicular nuclei. The portal tract showed dilated irregular portal vein filled with blood, necrotic tissue (red arrow), focal necrosis in some hepatocytes with increased eosinophilia and nuclear disappearance and a ductal reaction (new bile duct formation) at the periphery of the portal tract with periportal fibrosis. (**C**) STZ + Dapg showing moderate hepatotoxicity in the form of partial degeneration of hepatic tissue with necrotic nuclei (black arrow) with bleeding (green arrow) (H&EX400). (**D**) STZ + Zn–Dapg-treated group showing great amelioration in the hepatic structure with mild bleeding and red blood cells (orange arrow) (H&EX400). (**E**) STZ + Cr–Dapg showing very mild toxicity in the form of hypertrophy of hepatocytes with some binucleated hepatocytes (black arrow) that contained mild brown particles of bilirubin indicating biliary tract obstruction (black arrow), focal necrosis of some hepatocytes (red arrow) and mild ductal reactions at the periphery of the central vein (H&EX400). (**F**) STZ + Se–Dapg showing very mild toxicity in the form of hypertrophy of hepatocytes with granular eosinophilic cytoplasm, with mild congested central vein (***), ballooning degeneration in some hepatocytes (red arrow) and focal and single hepatocyte necrosis (green arrow).

4. Discussion

Dapg treatment can greatly control type II DM by improving glycemic control, reducing hepatic fat accumulation, maintaining normal liver size and elevating the hepatic insulin level in the blood [41]. Thus, the current study is of great importance considering the clinically high importance of controlling blood glucose levels and ameliorating hepatic functions using Dapg with metals, including Zn, Cr and Se.

Different clinical trials for patients with DM have been conducted. These studies found a significant decline in aspartate aminotransferase (AST) and alanine aminotransferase (ALT) levels following the administration of Dapg. Previous studies concluded that such reductions were also seen in the glycemic values, which is similar to the results of the current study. However, in this study, it was found that Dapg novel metal complexes induced a greater reduction in hepatic transaminases and amelioration of the glycemic state as sitagliptin previous findings and concepts [42].

In accordance with the results of the current study, previous studies reported that Dapg induced an improvement in liver enzymes (ALT or AST) and such improvements could induce a reduction in insulin resistance [43], thereby ameliorating the homeostatic model assessment for insulin resistance. This indicates a direct effect of Dapg on the inflammatory profile of hepatic tissues. These results support the findings regarding the high improvement induced by the Dapg novel metal complexes. In addition, these metal conjugations with Dapg induced additional improvements in the drug characteristics [44].

The effects of SGLT2 on improving fat accumulation in the hepatic tissues have been reported. Previous studies reported a reduction in hepatic triglycerides and a decline in hepatic fibrosis [45]. In the current study, treatment with Dapg elicited a moderately significant alteration in hepatic indicators. Meanwhile, treatment with Dapg novel metal complexes with either Cr, Zn and Se ameliorated hepatic injury and suppressed oxidative stress [46–48]. The amelioration of biochemical hepatic functions with novel complexes is important, as [49] demonstrated that excessive lipid accumulation can lead to cellular injury and death, and this strengthens the role of Dapg metal complexes in the protection of hepatic functions and reduction of lipid accumulation.

Parallel to the current findings, treatment of *db*/*db* male mice with Dapg for one month significantly reduced blood glucose levels in the circulation and increased glucose excretion in the urine. These observations were associated with reduced progression of albuminuria and inflammation [50]. Additionally, liver markers of inflammation, liver enzymes, oxidative stress markers and fat content were also reduced by Dapg treatment, and the success point of our current study is that we confirmed the previously obtained results for Dapg and its additional hepatoprotective effect and higher antioxidant defense capacities against oxidative stress in the case of treatment with Dapg with either Cr, Zn and Se. A great hepatic function improvement was recorded in the Se–Dapg-treated group and this confirms the ability of Se to enhance the activity of Dapg, as reported for the role of Se in hepatic protection [51].

Lipid peroxidation is suppressed by the release of some important antioxidant enzymes, such as glutathione [52]. Glutathione plays an essential antioxidative role against excessive reactive oxygen species [53]. In the current study, a marked alteration in either glutathione reductase (GRx) or GPx levels was observed in the STZ-induced diabetic rats. Meanwhile, these parameters were improved in the diabetic rats treated with the Dapg novel metal complexes.

MDA is an essential marker for the induction of lipid peroxidation [54]. In the current study, DM caused the elevation of MDA levels. The biological and pharmacological activities of the novel complexes of Dapg with Zn, Cr and/or Se ameliorated the hepatic functions and rejuvenated the antioxidant defense system [55]. The present study demonstrated that DM induced hepatotoxicity and severe oxidative stress, which could be mitigated by the administration of Dapg metal complexes with Zn, Cr and/or Se. The Dapg metal complexes also improved the hepatic structure more than Dapg alone.

To confirm the finding that Cr with Dapg ameliorates the blood glucose level, a previous study revealed that Cr with antidiabetic drugs caused a significant decline in the blood glucose level in alloxan-induced diabetic rats as compared to non-treated diabetic rats [56].

Reactive oxygen species, such as free radicals, play essential roles in the progression of STZ-induced experimental DM, as well as in the triggering of severe oxidative injury [57]. Under excessive oxidative stress conditions, reactive oxygen species directly participate in the induction of many diseases [52]. The human body is well equipped with many antioxidant enzymes, such as SOD, CAT and glutathione (GPx and GRx) [58]. The generation of high levels of free radicals can result in severe oxidative tissue or organ injuries [57].

People who have had diabetes for a long time may have peripheral nerve damage and reduced blood flow to their extremities, which increases the chance of bacterial infection. The high sugar levels in their blood and tissues allow bacteria to grow and allow infections to develop more quickly, which will eventually affect all the organs of the body [59]. The findings of current study showed that complexes of Dapg with Zn, Cr and Se contributed to the lowering of blood glucose levels in treated groups, which is of great importance for diabetics, and these complexes also showed high antibacterial activity against different types of bacterial strains related to the digestive system and its physiological functions, such as *Escherichia coli* and *Bacillus subtilis*. Moreover, a point of novelty and importance is the antibacterial activity of Zn–Dapg against *Streptococcus pneumonia*, which is of great importance for the protection of diabetics, especially during the COVID-19 pandemic.

The current study showed an improvement in the hepatic functions and antioxidant defense system in the group treated with the Dapg novel complexes. These effects were indicated by significant reductions in portal inflammatory cell infiltration and hemorrhage.

5. Conclusions

The present study provides new information on novel complexes of Dapg with Zn, Cr and/or Se and their potent hepatoprotective effects against STZ-induced experimental DM and hepatic injury. The novel Dapg metal complexes prevented histopathological alterations in DM and inhibited the excessive triggering of reactive oxygen species that induced oxidative injury in diabetic male rats. In addition, the Cr–Dapg complex upregulated the hepatic antioxidant defense system, thereby preventing severe oxidative injury. Therefore, Dapg novel complexes may be considered potent agents for attenuating the hepatic injury and pathophysiological complications of DM. In fact, chronic liver disease is an emerging risk factor for increased mortality due to COVID-19 [60]. As the COVID-19 pandemic continues, these new data may provide a potential tool to reduce mortality, and clinical studies are recommended.

Author Contributions: Conceptualization, S.M.E.-M., E.H.A.-T., R.A.A.-E., S.H.Q. and R.Z.H.; methodology, S.M.E.-M., E.H.A.-T., S.H.Q. and R.Z.H.; validation, S.M.E.-M. and R.Z.H.; formal analysis, S.M.E.-M., E.H.A.-T., S.H.Q., R.A.A.-E. and R.Z.H.; investigation, S.M.E.-M. and R.Z.H.; resources, S.M.E.-M., E.H.A.-T., S.H.Q. and R.Z.H.; data curation, S.M.E.-M., E.H.A.-T., S.H.Q., R.A.A.-E. and R.Z.H.; writing—original draft preparation, S.M.E.-M., S.H.Q. and R.Z.H.; writing—review and editing, S.M.E.-M., E.H.A.-T., S.H.Q., R.A.A.-E. and R.Z.H.; supervision, S.M.E.-M., E.H.A.-T., S.H.Q., R.A.A.-E. and R.Z.H.; project administration, S.M.E.-M. and R.Z.H.; funding acquisition, S.M.E.-M., E.H.A.-T., S.H.Q., R.A.A.-E. and R.Z.H. All authors have read and agreed to the published version of the manuscript.

Funding: This research received no external funding.

Institutional Review Board Statement: The study was conducted according to the guidelines of the Declaration of Helsinki and approved by the Ethics Committee of the Deanship of Scientific Research in Taif University.

Informed Consent Statement: Not applicable.

Data Availability Statement: Data analyzed or generated during this study are included in this manuscript.

Acknowledgments: Authors acknowledge to Taif University Researchers Supporting Project number (TURSP-2020/21), Taif University, Taif, Saudi Arabia.

Conflicts of Interest: The authors declare no conflict of interest.

References

1. Aktar, F.; Sultan, Z.; Rashid, M.A. Chromium (III) Complexes of Metformin, Dapagliflozin, Vildagliptin and Glimepiride Potentiate Antidiabetic Activity in Animal Model. *Int. J. Curr. Res. Rev.* **2021**, *13*, 64–69. [CrossRef]
2. Hippisley-Cox, J.; Coupland, C. Diabetes treatments and risk of amputation, blindness, severe kidney failure, hyperglycaemia, and hypoglycaemia: Open cohort study in primary care. *Br. Med. J.* **2016**, *352*, 1450. [CrossRef]
3. Chaudhury, A.; Duvoor, C.; Reddy Dendi, V.S.; Kraleti, S.; Chada, A.; Ravilla, R.; Marco, A.; Shekhawat, N.S.; Montales, M.T.; Kuriakose, K.; et al. Clinical Review of Antidiabetic Drugs: Implications for Type 2 Diabetes Mellitus Management. *Front. Endocrinol.* **2017**, *8*, 6. [CrossRef] [PubMed]
4. Thongnaka, L.; Chatsudthipongb, V.; Kongkaewc, A.; Lungkaphin, A. Effects of dapagliflozin and statins attenuate renal injury and liver steatosis inhigh-fat/high-fructose diet-induced insulin resistant rats. *Toxicol. Appl. Pharmacol.* **2020**, *396*, 114997. [CrossRef] [PubMed]
5. Merovci, A.; Solis-Herrera, C.; Daniele, G.; Eldor, R.; Fiorentino, T.V.; Tripathy, D.; Xiong, J.; Perez, Z.; Norton, L.; Abdul-Ghani, M.A.; et al. Dapagliflozin improves muscle insulin sensitivity but enhances endogenous glucose production. *J. Clin. Investig.* **2014**, *124*, 509–514. [CrossRef]
6. Belosludtsev, K.N.; Starinets, V.S.; Belosludtsev, M.N.; Mikheeva, I.B.; Dubinin, M.V.; Belosludtseva, N.V. Chronic treatment with dapagliflozin protects against mitochondrial dysfunction in the liver of C57BL/6NCrl mice with high-fat diet/ streptozotocin-induced diabetes mellitus. *Mitochondrion* **2021**, *59*, 246–254. [CrossRef] [PubMed]
7. Dos Santos, L.R.; Filho, R.B. Treatment of nonalcoholic fatty liver disease with dapagliflozin in non-diabetic patients. *Metab. Open* **2020**, *5*, 100028. [CrossRef]
8. Refat, M.S.; El-Megharbel, S.M.; Hussien, M.A.; Hamza, R.Z.; Al-Omar, M.A.; Naglah, A.M.; Afifi, W.M.; Kobeasy, M.I. Spectroscopic, structural characterizations and antioxidant capacity of the chromium (III) niacinamide compound as a diabetes mellitus drug model. *Spectrochim. Acta Part A Mol. Biomol. Spectrosc.* **2017**, *173*, 122–131. [CrossRef]
9. El-Megharbel, S.M.; Alsawat, M.; Al-Salmi, F.A.; Hamza, R.Z. Utilizing of (Zinc Oxide Nano-Spray) for Disinfection against "SARS-CoV-2" and Testing Its Biological Effectiveness on Some Biochemical Parameters during (COVID-19 Pandemic)—"ZnO Nanoparticles Have Antiviral Activity against (SARS-CoV-2)". *Coatings* **2021**, *11*, 388. [CrossRef]
10. Grüngreiff, K.; Reinhold, D.; Wedemeyer, H. The role of zinc in liver cirrhosis. *Ann. Hepatol.* **2016**, *15*, 7–16. [CrossRef]
11. El-Megharbel, S.M.; Al-Salmi, F.A.; Al-Harthi, S.; Alsolami, K.; Hamza, R.Z. Selenium/Chitosan-Folic Acid Metal Complex Ameliorates Hepatic Damage and Oxidative Injury in Male Rats Exposed to Sodium Fluoride. *Crystals* **2021**, *11*, 1354. [CrossRef]
12. El-Megharbel, S.M.; Al-Salmi, F.A.; Al-Harthi, S.; Alsolami, K.; Hamza, R.Z. Chitosan/Selenium Nanoparticles Attenuate Diclofenac Sodium-Induced Testicular Toxicity in Male Rats. *Crystals* **2021**, *11*, 1477. [CrossRef]
13. Abu-El-Zahab, H.S.H.; Hamza, R.Z.; Montaser, M.M.; El-Mahdi, M.M.; Al-Harthi, W.A. Antioxidant, antiapoptotic, antigenotoxic, and hepatic ameliorative effects of L-carnitine and selenium on cadmium-induced hepatotoxicity and alterations in liver cell structure in male mice. *Ecotoxicol. Environ. Saf.* **2019**, *173*, 419–428. [CrossRef]
14. Tuerk, M.J.; Fazel, N. Zinc deficiency. *Curr. Opin. Gastroenterol.* **2009**, *25*, 136–143. [CrossRef] [PubMed]
15. Hazem, R.M.; Ibrahim, A.Z.; Ali, D.A.; Moustafa, Y.M. Dapagliflozin improves steatohepatitis in diabetic rats via inhibition of oxidative stress and inflammation. *Int. Immunopharmacol.* **2022**, *104*, 108503. [CrossRef] [PubMed]
16. Li, L.; Li, Q.; Huang, W.; Han, Y.; Tan, H.; An, M.; Xiang, Q.; Zhou, R.; Yang, L.; Cheng, Y. Dapagliflozin Alleviates Hepatic Steatosis by Restoring Autophagy via the AMPK-mTOR Pathway. *Front. Pharmacol.* **2021**, *12*, 589273. [CrossRef]
17. Al-Salmi, F.A.; Hamza, R.Z. Efficacy of Vanadyl Sulfate and Selenium Tetrachloride as Anti-Diabetic Agents against Hyperglycemia and Oxidative Stress Induced by Diabetes Mellitus in Male Rats. *Curr. Issues Mol. Biol.* **2022**, *44*, 94–104. [CrossRef]
18. Hamza, R.Z.; Al-Motaani, S.E.; Al-Talhi, T. Therapeutic and Ameliorative Effects of Active Compounds of *Combretum molle* in the Treatment and Relief from Wounds in a Diabetes Mellitus Experimental Model. *Coatings* **2021**, *11*, 324. [CrossRef]
19. Ohkawa, H.; Ohishi, N.; Yagi, K. Assay for lipid peroxides in animal tissues by thiobarbituric acid reaction. *Anal. Biochem.* **1979**, *95*, 351. [CrossRef]
20. Marklund, S.; Marklund, G. Involvement of the superoxide anion radical in the autoxidation of pyrogallol and a convenient assay for superoxide dismutase. *Eur. J. Biochem.* **1974**, *47*, 469–474. [CrossRef]
21. Aebi, H. Catalase in vitro. *Meth. Enzymol.* **1984**, *105*, 121–126.
22. Couri, D.; Abdel-Rahman, M.S. Effect of chlorine dioxide and metabolites on glutathione-dependent system in rat, mouse and chicken blood. *J. Environ. Pathol. Toxicol.* **1980**, *3*, 451–460.
23. Hafeman, D.G.; Sunde, R.A.; Hoekstra, W.G. Effect of dietary selenium on erythrocyte and liver glutathione peroxidase in the rat. *J. Nutrit.* **1974**, *104*, 580–587. [CrossRef] [PubMed]
24. Nachnani, J.S.; Bulchandani, D.G.; Nookala, A.; Herndon, B.; Molteni, A.; Pandya, P.; Taylor, R.; Quinn, T.; Weide, L.; Alba, L.M. Biochemical and histological effects of exendin-4 (exenatide) on the rat pancreas. *Diabetologia* **2010**, *53*, 153–159. [CrossRef]

25. Bauer, A.W.; Kirby, W.M.; Sherris, C.; Turck, M. Antibiotic susceptibility testing by a standardized single disc method. *Am. J. Clin. Pathol.* **1966**, *45*, 493. [CrossRef] [PubMed]
26. Pfaller, M.A.; Burmeister, L.; Bartlett, M.A.; Rinaldi, M.G. Multicenter evaluation of four methods of yeast inoculum preparation. *J. Clin. Microbiol.* **1988**, *26*, 1437–1441. [CrossRef] [PubMed]
27. *M100*; Performance Vol. Antimicrobial Susceptibility of Flavobacteria. National Committee for Clinical Laboratory Standards: Wayne, PA, USA, 1997.
28. *Approved Standard M7-A3*; Methods for Dilution Antimicrobial Susceptibility Tests for Bacteria That Grow Aerobically. National Committee for Clinical Laboratory Standards: Villanova, PA, USA, 1993.
29. Liebowitz, L.D.; Ashbee, H.R.; Evans, E.G.V.; Chong, Y.; Mallatova, N.; Zaidi, M.; Gibbs, D. A two year global evaluation of the susceptibility of Candida species to fluconazole by disk diffusion, *Diagn. Microbiol. Infect. Dis.* **2001**, *40*, 27–33. [CrossRef]
30. Matar, M.J.; Ostrosky-Zeichner, L.; Paetznick, V.L.; Rodriguez, J.R.; Chen, E.; Rex, J.H. Correlation between E-test, disk diffusion, and microdilution methods for antifungal susceptibility testing of fluconazole and voriconazole. *Antimicrob. Agents Chemother.* **2003**, *47*, 1647–1651. [CrossRef]
31. Petrie, A.; Sabin, C. *Medical Statistics at a Glance*, 3rd ed.; Wiley-Blackwell: Hoboken, NJ, USA, 2009; Volume 23. [CrossRef]
32. Burger, K. *Coordination Chemistry: Experimental Methods*; Butterworth Group: London, UK, 1973.
33. Gunasekaran, S.; Kumar, R.T.; Ponnusamy, S. Vibrational spectra and normal coordinate analysis of adrenaline and dopamine. *Indian J. Pure Appl. Phys.* **2007**, *45*, 884.
34. Miháliková, I.; Friák, M.; Jirásková, Y.; Holec, D.; Koutná, N.; Šob, M. Impact of Nano-Scale Distribution of Atoms on Electronic and Magnetic Properties of Phases in Fe-Al Nanocomposites: An Ab Initio Study. *Nanomaterials* **2018**, *8*, 1059. [CrossRef] [PubMed]
35. Refat, M.S. Complexes of uranyl(II), vanadyl(II) and zirconyl(II) with orotic acid "vitamin B13": Synthesis, spectroscopic, thermal studies and antibacterial activity. *J. Mol. Struct.* **2007**, *842*, 24. [CrossRef]
36. Bellamy, L.J. *The Infrared Spectra of Complex Molecules*; Chapman and Hall: London, UK, 1975.
37. Oztürk, O.F.; Şekerci, M.; Ozdemir, E. Synthesis of 5, 6-O-Cyclohexylidene-l-amino-3-azahexane and Its Co (II), Ni (II), and Cu (II) Complexes. *Russ. J. Coord. Chem.* **2005**, *31*, 687–690. [CrossRef]
38. Drago, R.S.; Meek, D.W.; Joosten, M.S.; Laroche, L. Spectrochemical studies of a series of amides as ligands with nickel (II) and chromium (III). *Inorg. Chem.* **1963**, *2*, 124. [CrossRef]
39. Nakamoto, K. *Infrared and Raman Spectra of Inorganic and Coordination Compounds*; Wiely: New York, NY, USA, 1978.
40. Cullity, B.D. *Elements of X-ray Diffraction*, 2nd ed.; Addision-Wesley Publishing Company: Boston, MA, USA, 1978.
41. Kurinami, N.; Sugiyama, S.; Yoshida, A.; Hieshima, K.; Miyamoto, F.; Kajiwara, K.; Jinnouch, K.; Jinnouchi, T.; Jinnouchi, H. Dapagliflozin significantly reduced liver fat accumulation associated with a decrease in abdominal subcutaneous fat in patients with inadequately controlled type 2 diabetes mellitus. *Diabetes Res. Clin. Pract.* **2018**, *142*, 254–263. [CrossRef]
42. SM El-Megharbel, MS Refat, FA Al-Salmi, RZ Hamza. In Situ Neutral System Synthesis, Spectroscopic, and Biological Interpretations of Magnesium(II), Calcium(II), Chromium(III), Zinc(II), Copper(II) and Selenium(IV) Sitagliptin Complexes. *Int. J. Environ. Res. Public Health* **2021**, *18*, 8030. [CrossRef] [PubMed]
43. Ismail, H.A.; Hamza, R.Z.; El-Shenawy, N.S. Potential protective effects of blackberry and quercetin on sodium fluoride induced impaired hepatorenal bi-omarkers, sex hormones and hematotoxicity in male rats. *J. Appl. Life Sci. Int.* **2014**, *1*, 1–16. [CrossRef]
44. Goh, G.B.; McCullough, A.J. Natural history of nonalcoholic fatty liver disease. *Dig. Dis. Sci.* **2016**, *61*, 1226–1233. [CrossRef]
45. Akuta, N.; Watanabe, C.; Kawamura, Y.; Arase, Y.; Saitoh, S.; Fujiyama, S.; Sezaki, H.; Hosaka, T.; Kobayashi, M.; Kobayashi, M.; et al. Effects of a sodium–glucose cotransporter 2 inhibitor in nonalcoholic fatty liver disease complicated by diabetes mellitus: Preliminary prospective study based on serial liver biopsies. *Hepatol. Commun.* **2017**, *1*, 46–52. [CrossRef]
46. Nakano, S.; Katsuno, K.; Isaji, M.; Nagasawa, T.; Buehrer, B.; Walker, S.; Wikison, W.O.; Cheatham, B. Remogliflozin etabonate improves fatty liver disease in diet-induced obese male mice. *J. Clin. Exp. Hepatol.* **2015**, *5*, 190–198. [CrossRef]
47. Jojima, T.; Tomotsune, T.; Iijima, T.; Akimoto, K.; Suzuki, K.; Aso, Y. Empagliflozin (an SGLT2 inhibitor), alone or in combination with linagliptin (a DPP-4 inhibitor), prevents steatohepatitis in a novel mouse model of non-alcoholic steatohepatitis and diabetes. *Diabetol. Metab. Syndr.* **2016**, *8*, 45. [CrossRef] [PubMed]
48. Ekholm, E.; Hansen, L.; Johnsson, E.; Iqbal, N.; Carlsson, B.; Chen, H.; Hirshberg, B. Combined treatment with saxagliptin plus dapafliflozin reduces insulin levels by increased insulin clearance and improves b-cell function. *Endocr. Pract.* **2017**, *23*, 258–265. [CrossRef] [PubMed]
49. Obara, K.; Shirakami, Y.; Maruta, A.; Ideta, T.; Miyazaki, T.; Kochi, T.; Sakai, H.; Tanaka, T.; Seishima, M.; Shimizu, M. Preventive effects of the sodium glucose cotransporter 2 inhibitor tofogliflozin on diethylnitrosamine-induced liver tumorigenesis in obese and diabetic mice. *Oncotarget* **2017**, *8*, 58353–58363. [CrossRef]
50. Li, Y.; Zhang, Y.; Ji, G.; Shen, Y.; Zhao, N.; Liang, Y.; Wang, Z.; Liu, M.; Lin, L. Autophagy Triggered by Oxidative Stress Appears to Be Mediated by the AKT/mTOR Signaling Pathway in the Liver of Sleep-Deprived Rats. *Oxidative Med. Cell Longev.* **2020**, *2020*, 6181630. [CrossRef] [PubMed]
51. Tang, L.; Wu, Y.; Sjöström, M.T.D.; Johansson, U.; Peng, X.; Smith, D.M.; Huang, Y. Dapagliflozin slows the progression of the renal and liver fibrosis associated with type 2 diabetes. *Am. J. Physiol. Endocrinol. Metab.* **2017**, *313*, E563–E576. [CrossRef]

52. Hamza, R.Z.; El-Megharbel, S.M.; Altalhi, T.; Gobouri, A.A.; Alrogi, A.A. Hypolipidemic and hepatoprotective synergistic effects of selenium nanoparticles and vitamin. E against acrylamide-induced hepatic alterations in male albino mice. *Appl. Organomet. Chem.* **2020**, *34*, e5458. [CrossRef]
53. Hamza, R.Z.; Al-Harbi, M.S. Amelioration of paracetamol hepatotoxicity and oxidative stress on mice liver with silymarin and Nigella sativa extract supplements. *Asian Pac. J. Trop. Biomed.* **2015**, *5*, 521–531. [CrossRef]
54. Refat, M.S.; Hamza, R.Z.; Adam, A.M.A.; Saad, H.A.; Gobouri, A.A.; Al-Harbi, F.S.; Al-Salmi, F.A.; Altalhi, T.; El-Megharbel, S.M. Quercetin/Zinc complex and stem cells: A new drug therapy to ameliorate glycometabolic control and pulmonary dysfunction in diabetes mellitus: Structural characterization and genetic studies. *PLoS ONE* **2021**, *16*, e0246265. [CrossRef] [PubMed]
55. Rahman, F.; Salam, M.A.; Rahman, A.; Sultan, M.Z. Studies of interactions of valsartan, glimepiride and ciprofloxacin HCl by DSC and HPLC. *Bangl. Pharm. J.* **2017**, *20*, 195–200. [CrossRef]
56. Al-Baqami, N.; Hamza, R. Synergistic antioxidant capacities of vanillin and chitosan nanoparticles against reactive oxygen species, hepatotoxicity, and genotoxicity induced by aging in male Wistar rats. *Hum. Exp. Toxicol.* **2021**, *40*, 183–202. [CrossRef] [PubMed]
57. Refat, M.S.; Hamza, R.Z.; Adam, A.M.A.; Saad, H.A.; Gobouri, A.A.; Azab, E.; Al-Salmi, F.A.; Altalhi, T.A.; Khojah, E.; Gaber, A.; et al. Antioxidant, antigenotoxic, and hepatic ameliorative effects of quercetin/zinc complex on cadmium-induced hepatotoxicity and alterations in hepatic tissue structure. *Coatings* **2021**, *11*, 501. [CrossRef]
58. Hamza, R.Z.; Diab, A.E.A.A. Testicular protective and antioxidant effects of selenium nanoparticles on Monosodium glutamate-induced testicular structure alterations in male mice. *Toxicol. Rep.* **2020**, *7*, 254–260. [CrossRef] [PubMed]
59. Juliana, C.; Janine, C.; Cresio, A. Infections in patients with diabetes mellitus: A review of pathogenesis. *Indian J. Endocrinol. Metab.* **2012**, *16* (Suppl. 1), S27–S36.
60. Galiero, R.; Pafundi, P.C.; Simeon, V.; Rinaldi, L.; Perrella, A.; Vetrano, E.; Caturano, A.; Alfano, M.; Beccia, D.; Nevola, R.; et al. Impact of chronic liver disease upon admission on COVID-19 in-hospital mortality: Findings from COVOCA study. *PLoS ONE* **2020**, *15*, e0243700. [CrossRef] [PubMed]